3-4 Ionospheric Variations and Coupling with the Middle and Lower Atmosphere

3-4-1 Ionospheric Wavenumber 4 Longitudinal Structure

JIN Hidekatsu and SAGAWA Eiichi

Recent satellite-based remote sensing observations have revealed the existence of an ionospheric wavenumber 4 longitudinal structure. It had been known that a region of the lower atmosphere having active cumulus convection is split in the longitudinal direction depending on land-sea distributions, from which atmospheric waves giving the appearance of being wavenumber 4 are formed (when viewed from a fixed local time perspective). The discovery of the wavenumber 4 structure eloquently suggests the possibility of lower atmospheric activity affecting the ionosphere and has since driven a number of studies, including those based on observations and simulations, to probe into the process of atmosphere-ionosphere coupling. This paper introduces the starting point of these studies-the observation of a wavenumber 4 structure. It proceeds to introduce a numerical simulation that reproduces a wavenumber 4 structure and discusses the mechanism of atmosphere-ionosphere coupling in the wavenumber 4 structure.

Keywords
Ionosphere, Troposphere, Atmosphere-ionosphere coupling, Atmospheric wave, Ionospheric dynamo

1 Introduction: Ionospheric latitudinal and longitudinal structures

The ionosphere is formed as the background neutral atmosphere becomes ionized upon exposure to solar ultraviolet light. Accordingly, the distribution of ionospheric density depends on latitude, longitude, and local time according to the distribution of neutral atmospheric density and the intensity of solar radiation. As for latitudinal distributions, a characteristic structure known as an "equatorial ionization anomaly (EIA)" is also in place. The term EIA refers to a structure in which peaks in ionospheric density are latitudinally divided across the magnetic equator, not located right above the equator having an intense level of solar radiation, and the structure was originally detected by the Japanese from ionosonde observations[1]. The cause of EIA is closely related to an electric field generated in the ionospheric dynamo process, as detailed in Reference[2] of this feature article. Figure 1 shows an EIA caught by remote-sensing far ultraviolet light from the *IMAGE* satellite[3]. The EIA shown in Fig. 1 is a nighttime airglow observation, though it is generated in the morning and lasts until after sunset.

Longitudinal distributions of ionospheric density (when viewed with local time fixed) will not be manifested in ionization (provided the background neutral atmosphere has a low dependence on longitude). Some studies on longitudinal distributions that have examined

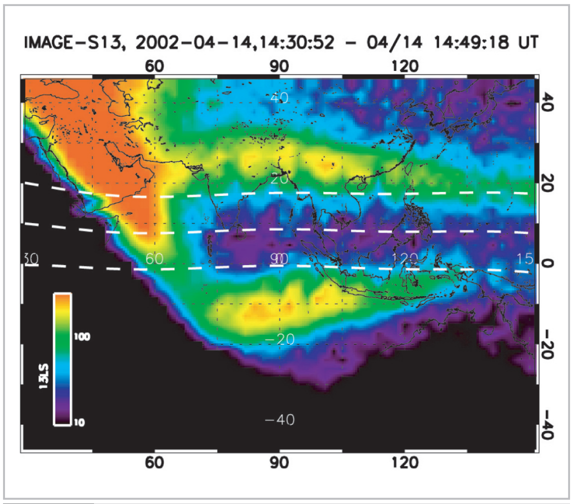

Fig. 1 *Equatorial ionization anomaly (EIA) caught by observing far ultraviolet light from the IMAGE spacecraft* [3]

An EIA caught by remote-sensing far ultraviolet light from the IMAGE spacecraft[3] Averages at 14:30 to 14:49 UT (Universal Time) on April 14, 2002. The three white lines (from top to bottom) designate the positions at geomagnetic latitudes of +10 degrees, 0 degrees, and -10 degrees, respectively. The nighttime airglow that appears latitudinally divided in the center of the diagram points to an EIA. The bright area in the upper-left part of the diagram encloses an area exposed to daytime solar radiation; the black area from the left-side center downward marks an area beyond the field of vision of the observation equipment.

the longitudinal dependence of equatorial anomalies from ionosonde observations cite the complex geometry of the geomagnetic field, namely, the difference between the geographic equator and the magnetic equator, the geomagnetic field's angle of deviation (i.e., difference between the geographic north pole and magnetic north), longitudinal dependence of magnetic field intensity, and other factors as being responsible for the longitudinal dependence of equatorial anomalies[4]. Based on recent satellite observations, longitudinal dependence could not be explained by the magnetic field geometry alone, and other effects accounting for this dependence must be explored.

This paper introduces a wavenumber 4 ionospheric longitudinal structure that was recently spotted by satellite remote-sensing observations (Chapter **2**). The discovery of this wavenumber 4 structure eloquently suggests the possibility of lower atmospheric activity affecting the ionosphere, and has since encouraged a number of studies. Chapter **3** discusses the relation between the ionospheric wavenumber 4 structure and the lower atmospheric moist convection. Lastly, Chapter **4** introduces a numerical simulation that reproduces a wavenumber 4 structure and discusses the physical mechanism of atmosphere-ionosphere coupling in the wavenumber 4 structure.

2 Wavenumber 4 longitudinal structure discovered by satellite remote sensing

Figure 2 shows the longitudinal distribution of EIA derived by extracting data for the same local time (2200 to 2300 hours LT) from far ultraviolet light observations (wavelength 135.6 nm) conducted by the *IMAGE* spacecraft as mentioned earlier[3]. Given the satellite's orbit, the data availability was limited to the Northern Hemisphere. The axis of ordinate represents the magnetic latitude, though sufficient observation data in the vicinity of 300 degrees longitude was not available, since the magnetic equator sizably shifts southward at these locations. In Fig. 2, the intense airglow observed at 10 to 20 degrees magnetic latitude corresponds to the EIA crests (i.e., the region having the highest density in the latitudinal distribution). As for the longitudinal distributions of EIA, crests have intense airglow in the vicinity of 20, 120 and 230 degrees longitude, and weak airglow around 60, 150 and 250 degrees longitude, at longitude intervals of wavenumber 4. Crests having intense airglow are located at higher latitudes, with a high crest-to-trough (lowest-density area in the vicinity of the magnetic equator) airglow intensity ratio. This finding suggests that electric field variations relate to the longitudinal dependence of EIA.

Past studies of the longitudinal dependence of equatorial anomalies based on ground-based observations had not led to the discovery of an ionospheric wavenumber 4 structure due to insufficient longitude resolutions on a global scale. In the wake of the discovery of a wavenumber 4 structure by the IMAGE satellite, the presence of a wavenumber 4 structure in the ionospheric density distributions has been confirmed by observations from other satellites. These other satellites have also spotted a wavenumber 4 structure in the daytime, as well as at nighttime [5]. Wavenumber 4 structures have also been found in the background thermospheric atmosphere [6] and ionospheric current [7]. The ionospheric longitudinal structure has been found to vary from season to season, exhibiting a wavenumber 4 structure from spring, through summer, to autumn, but the wavenumber 4 structure gets blurred in winter (around December) to become a wavenumber 3 structure [8][9].

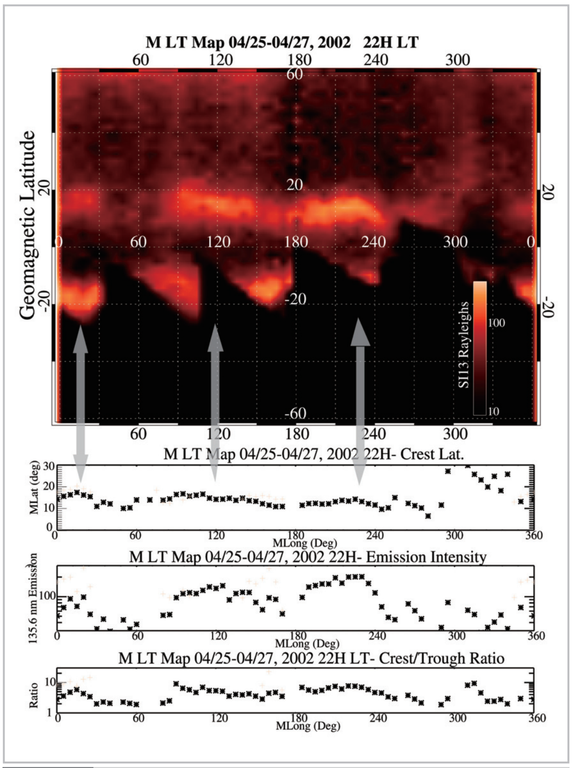

Fig.2 *Longitudinal structure of EIA caught by observing far ultraviolet light from the IMAGE spacecraft* [3]

The longitudinal structure of the EIA caught by remote-sensing far ultraviolet light from the *IMAGE* spacecraft [3]. Nighttime distributions (2200 to 2300 hours LT or local time) of the averages for April 25 to 27, 2002. The magnetic latitude is taken on the axis of ordinate. Due to the satellite's orbit, data on the Southern Hemisphere is missing. Observation data in the vicinity of 300 degrees longitude is also missing, since the magnetic equator sizably shifts southward at these locations. The three bottom panels plot the magnetic latitude of each crest (high-density area) in the EIA, the intensity of its airglow, and the crest-to-trough (low-density area) density ratio, respectively.

3 Relationship between ionospheric wavenumber 4 structure and lower atmospheric moist convection

The reason why an ionospheric wavenumber 4 structure attracts attention is that its origin is considered traceable to the lower atmosphere. Figure 3 shows yearly average rainfall distributions (diurnal component) estimated from cloud-top temperature measurements made by satellite observations [10]. As can be seen from Fig. 3, much rainfall is distributed in four regions: the low-latitude African Continent, Southeast Asia, the Pacific Ocean, and North America. In these regions with active moist convection, latent heat is released upon the formation of clouds and raindrops to energize the growth of atmospheric waves. The atmospheric waves induced by convective

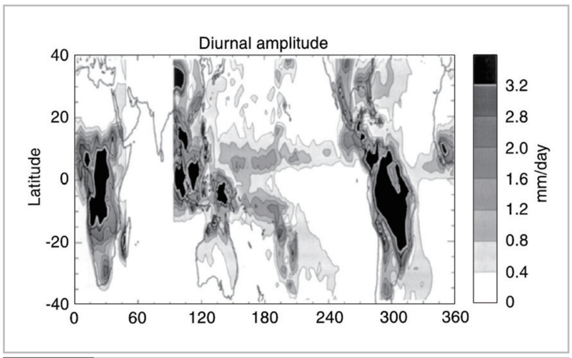

Fig.3 *Yearly average rainfall distributions (diurnal component) estimated from cloud-top temperature measurements* [10]

No satellite data is available for 50 to 90 degrees E longitude.

activity may propagate their energy from a troposphere located around an ionospheric height of 10 km to an upper atmospheric region at 100 km or higher to generate the ionospheric longitudinal structure. A study of atmospheric tides propagating as far as the thermospheric region, based on the rainfall distributions shown in Fig. 3, revealed the dominance of nonmigrating (i.e., non-sun-synchronously propagating) tides, especially DE3 (diurnal eastward propagating tide with zonal wavenumber 3), as well as migrating (i.e., sun-synchronously propagating) tides such as DW1 (diurnal westward propagating tide with zonal wavenumber 1)[10][11]. When viewed with the local time fixed, DE3 has wavenumber 4 longitudinal dependence, whereas DW1 has no longitudinal dependence, thereby suggesting its effect on the ionospheric longitudinal structure.

4 Ionospheric wavenumber 4 structure reproduced by numerical simulation and its formation mechanism

The discovery of the ionospheric wavenumber 4 structure entailed numerical simulations concerning the process of atmosphere-ionosphere coupling. Figure 4 presents the results of calculation made by an electrodynamic model introduced in Reference[2] that represent the distributions of vertical plasma drift driven by electric field (at ionospheric height of 300 km, 1200 hours LT). Neutral wind distributions as input to the electrodynamics model had been provided from the simulation output of an extended atmospheric general circulation model developed at Kyushu University and Tohoku University[13][14]. Although the wind velocity of the atmospheric general circulation model varied significantly from day to day (leading to day-to-day variation of electric field (plasma drift)), only the 30-day (September) average of the plasma drift is plotted in Fig. 4. Evidently from the figure, the plasma drift peaks in four regions: the low-latitude African Continent, Southeast Asia, the Pacific Ocean, and North America. Because east-west electric field (vertical plasma drift) on the equator is a driving source for EIA[2], the results of the electrodynamics model are linked to the wavenumber 4 longi-

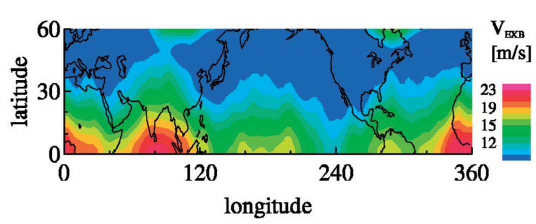

Fig.4 *Vertical plasma drift driven by electric field as reproduced by an electrodynamic model*

(30-day averages at an ionospheric height of 300 km, and the local time is fixed at 1200 LT)

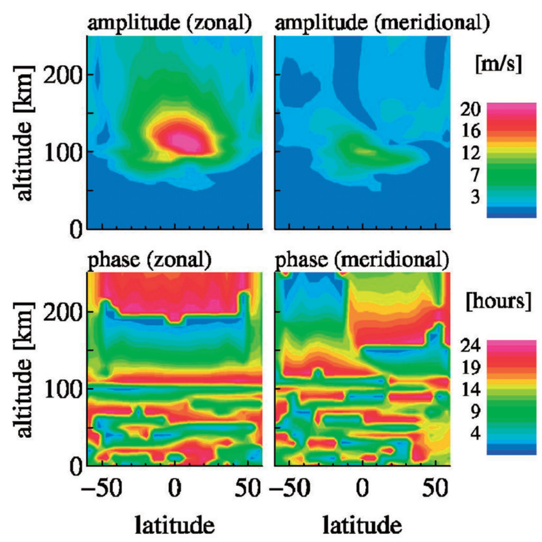

Fig.5 *Amplitude and phase of the DE3 tidal component extracted from results of the extended atmospheric general circulation model*[14]

Amplitude and phase of the DE3 (eastward propagating diurnal tide with zonal wavenumber-3) component extracted from results of the extended atmospheric general circulation model[14]

(Upper left: zonal (East-west) wind amplitude, lower left: zonal wind phase, upper right: meridional (north-south) wind amplitude, lower right: meridional wind phase) tudinal structure of EIA as reported in Reference[3].

Because the calculations shown in Fig. 4 use as an input the wind velocity derived from the atmospheric general circulation model without modification, the calculations include the contributions of all atmospheric waves reproduced by the atmospheric general circulation model. Chapter **3** stated that DE3—a nonmigrating tide excited in the lower atmosphere—becomes dominant in the thermosphere in September equinox. To examine the contribution of DE3 to the ionospheric wavenumber 4 structure and its formation mechanism, Reference[14] extracted migrating tidal components and DE3 from the distributions of wind velocity simulated by the atmospheric general circulation model, and use the tidal winds as an input to the electrodynamic model. Figure 5 shows the distributions of amplitude and phase of the DE3 component extracted based on the results of the atmospheric general circulation model. Tidal propagation from the lower atmosphere to the upper atmosphere is clearly evident. More-

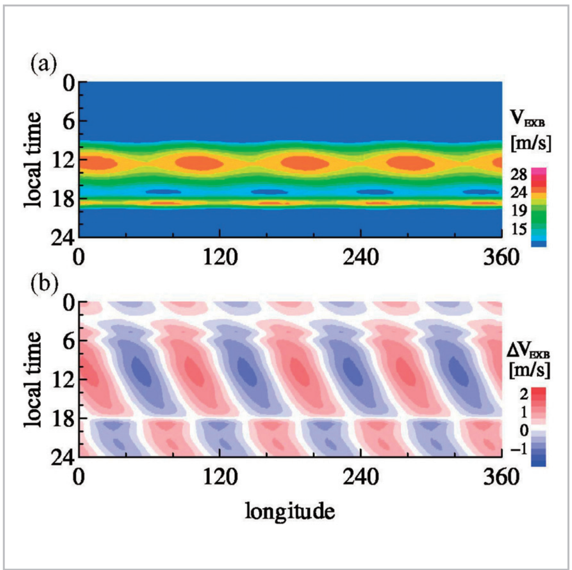

Fig.6 *Longitude-local time distributions of vertical plasma drift driven by dynamo electric field caused by the DE3 component* [14]

(a) Results of calculation by the electrodynamics model only using migrating tides and DE3 as input[14]. Longitude-local time distributions of vertical plasma drift driven by dynamo electric field at the height of 300 km

(b) The same as (a), but the contribution from migrating tides is removed to highlight only the contribution of the DE3 component.

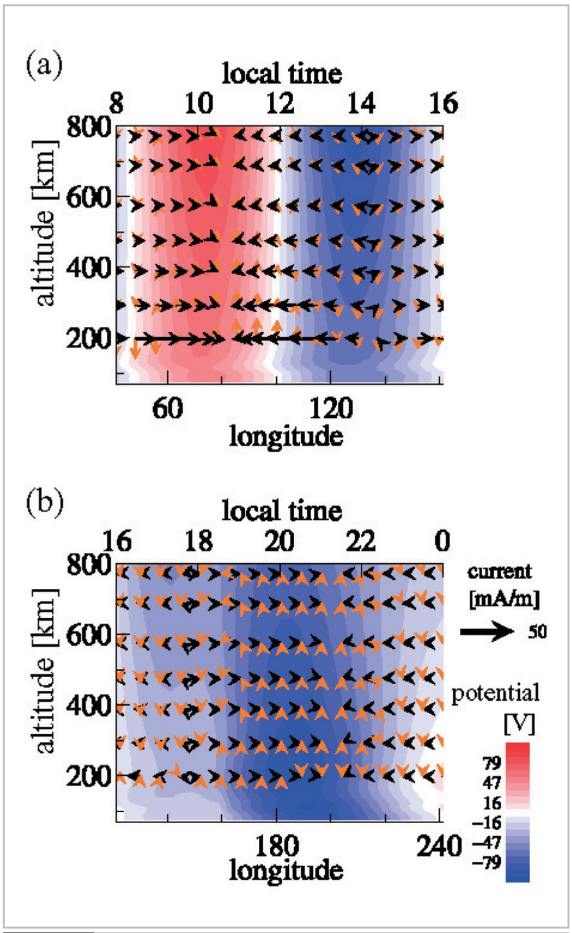

Fig.7 *Mechanism for the generation of zonal electric field variation as suggested by the electrodynamics model* [14]

The contour designates the longitude/local time-ionospheric height distributions of electrostatic potential (on the magnetic equatorial plane), with the arrow indicating the flow of dynamo current integrated along magnetic field lines (Hall current marked in black, Pedersen current in orange). These physical quantities only represent the contribution of the DE3 component.

(a) Snapshot taken at 05:20 UT (local time of 12 hours in the center of the diagram)

(b) Snapshot taken at 08:00 UT (local time of 20 hours in the center of the diagram) over, the east-west wind had large amplitude at the ionospheric dynamo region (around 110 km, where the conductivities are largest in their altitude profiles). In the dynamo region, the DE3 wind had uniform phase distribution in the latitude direction, which is an effective condition to the formation of dynamo electric field.

Figure 6 presents the longitude-local time distribution of vertical electric field drift in the plasma at an ionospheric height of 300 km as the results of calculation made by the electrodynamics model using migrating tides and DE3 as input. Only the contribution from DE3 is indicated in Fig. 6 (b). Evidently from Fig. 6, a wavenumber 4 structure has been formed by the DE3 in vertical electric field drift during the daytime. A wavenumber 4 structure has also been formed in the electric field drift after sunset, as well as during the daytime.

Figure 7 shows how DE3 creates a zonal electric field (vertical drift). As detailed in Reference[14], DE3 causes a zonal dynamo current to flow in the daytime, resulting in a positive charge being accumulated in the dynamo current convergent region (around 75 degrees longitude in Fig. 7 (a)), and a negative charge in the divergent region (around 135 degrees longitude in Fig. 7 (a)).Then, an eastward polarized electric field (upward vertical electric field drift) is formed between 75 and 135 degrees from the convergent region to the divergent region as shown in Fig. 7 (a). It intensifies the eastward background electric field in the daytime. Thus, DE3 promotes the growth of EIA at these longitudinal locations.

5 Conclusions

As introduced in this paper, the recently discovered ionospheric wavenumber 4 structure has been found to originate from the lower atmosphere. Other than the wavenumber 4 structure, phenomena suggesting a linkage from the lower atmosphere to the ionosphere have been suggested by a growing number of reports, thereby driving probes into the process of atmosphere-ionosphere coupling. Meteorological activities near the ground surface vary on many different spatial and temporal scales, with its impact possibly reaching as far as the remote upper ionosphere. Some day-to-day ionospheric variations relevant to space weather may also have some bearing on the lower atmosphere. To further advance probes into the process of atmosphere-ionosphere coupling, an integrated model of the Earth's whole atmospheric region covering from meteorological activities near the ground surface through the ionosphere would be necessary. To meet this need, major institutions in the U.S. and Japanese groups have embarked on the development of large-scale models to bolster further leaps in the implementation of such probes.

Acknowledgements

The numerical calculations described in Chapter **4** were implemented based on the calculation results of an extended atmospheric general circulation model developed at Kyushu University and Tohoku University. The author wishes to express deep appreciation to both universities.

References

1 Namba, S. and K. -I. Maeda, "Radio Wave Propagation," Corona, Tokyo, 1939.

2 Jin, H., "Ionospheric Dynamo Process," Special issue of this NICT Journal, 2–3–7, 2009.

3 Sagawa, E., T. J. Immel, H. U. Frey, and S. B. Mende, "Longitudinal structure of the equatorial anomaly in the nighttime ionosphere observed by IMAGE/FUV," J. Geophys. Res., Vol. 110, A11302, doi: 10.1029/2004JA010848, 2005.

4 Walker, G. O., "Longitudinal structure of the F-region equatorial anomaly: A review," J. Atmos. Terr. Phys., Vol. 43, p. 763, 1981.

5 Lin, C. H., C. C. Hsiao, J. Y. Liu, and C. H. Liu, "Longitudinal structure of the equatorial ionosphere: Time evolution of the four-peaked EIA structure," J. Geophys. Res., Vol. 112, A12305, doi: 10.1029/2007JA012455, 2007.

6 H. Liu, M. Yamamoto, and H. Lühr, "Wave- 4 pattern of the equatorial mass density anomaly: A thermospheric signature of tropical deep convection," Geophys. Res. Lett., Vol. 36, L18104, doi: 10.1029/2009GL039865, 2009.

7 Lühr, H., M. Rother, K. Häusler, P. Alken, and S. Maus, "The influence of nonmigrating tides on the longitudinal variation of the equatorial electrojet," J. Geophys. Res., Vol. 113, A08313, doi: 10.1029/2008JA013064, 2008.

8 Scherliess, L., D. C. Thompson, and R. W. Schunk, "Longitudinal variability of low-latitude total electron content: Tidal influences," J. Geophys. Res., Vol. 113, A01311, doi: 10.1029/ 2007JA012480, 2008.

9 Fejer, B. G., J. W. Jensen, and S. -Y. Su, "Quiet time equatorial F region vertical plasma drift model derived from ROCSAT-1 observations," J. Geophys. Res., Vol. 113, A05304, doi: 10.1029/2007JA012801, 2008.

10 Forbes, J. M., M. E. Hagan, X. Zhang, and K. Hamilton, "Upper atmosphere tidal oscillations due to latent heat release in the tropical troposphere," Ann. Geophysicae, Vol. 15, pp. 1165-1175, 1997.

11 Hagan, M. E., and J. M. Forbes, "Migrating and nonmigrating diurnal tides in the middle and upper atmosphere excited by tropospheric latent heat release," J. Geophys. Res., Vol. 107, p. 4754, doi: 10.1029/2001JD001236, 2002.

12 Miyoshi, Y., and H. Fujiwara, "Day-to-day variations of migrating diurnal tide simulated by a GCM from the ground surface to the exobase," Geophys. Res. Lett., Vol. 30, 1789, doi: 10.1029/2003GL017695, 2003.

13 Fujiwara, H., and Y. Miyoshi, "Characteristics of the large-scale traveling atmospheric disturbances during geomagnetically quiet and disturbed periods simulated by a whole atmosphere general circulation model," Geophys. Res. Lett., Vol. 33, L20108, doi: 10.1029/ 2006GL027103, 2006.

14 Jin, H., Y. Miyoshi, H. Fujiwara, and H. Shinagawa, "Electrodynamics of the formation of ionospheric wave number 4 longitudinal structure," J. Geophys. Res., Vol. 113, A09307, doi: 10.1029/2008JA013301, 2008.

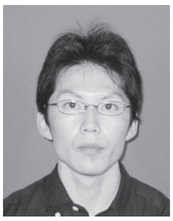

***JIN Hidekatsu**, Dr. Sci.*

Expert Researcher, Space Environment Group, Applied Electromagnetic Research Center

Upper Atmospheric Physics

***SAGAWA Eiichi**, Dr. Sci.*

Former : Senior Researcher, Space Weather Group, Applied Research and Standards Division

Space Weather